Organic &
Biomolecular
Chemistry

Cite this: *Org. Biomol. Chem.*, 2011, **9**, 4108

www.rsc.org/obc

PAPER

Click chemistry by microcontact printing on self-assembled monolayers: A structure–reactivity study by fluorescence microscopy†

Jan Mehlich and Bart Jan Ravoo*

Received 2nd February 2011, Accepted 14th March 2011
DOI: 10.1039/c1ob05187c

Microcontact printing (μCP) has developed into a powerful tool to functionalize surfaces with patterned molecular monolayers. μCP can also be used to induce a chemical reaction between a molecular ink and a self-assembled monolayer (SAM) in the nanoscale confinement between stamp and substrate. In this paper, we investigate the Huisgen 1,3-dipolar cycloaddition, the Diels–Alder cycloaddition and the thiol-ene/yne reaction induced by μCP. A range of fluorescent alkyne inks were printed on azide SAMs and fluorescence microscopy was used to monitor the extent of the 1,3-dipolar cycloaddition on a glass substrate. The rate of cycloaddition depends on the reactivity of the alkyne and on the presence of Cu(I). The cycloaddition is accelerated by Cu(I) but it also proceeds readily in the absence of Cu(I). In addition, a range of fluorescent diene inks were printed on alkene SAMs on glass. In this case, fluorescence microscopy was used to monitor the rate of the Diels–Alder cycloaddition as well as its retro-reaction. Finally, fluorescent thiol inks were printed on alkene SAMs on glass, and fluorescent alkenes and alkynes were printed on thiol SAMs. It is shown that reactions by μCP follow structure–reactivity relationships similar to solution reactions. Under optimized conditions all reactions lead to dense microarrays of addition products within minutes of printing time.

Introduction

The modification of inorganic surfaces with monolayers of organic molecules has found widespread application in nanofabrication, sensing, diagnostics and molecular electronics.[1–6] The microscale patterning of molecular monolayers is crucial to all of these applications. In recent years, microcontact printing (μCP) has developed into a powerful tool to functionalize substrates with spatially patterned molecular monolayers.[7–10] μCP is based on the selective transfer of ink molecules from a microstructured elastomeric stamp to a substrate in the contact area between stamp and substrate. μCP is commonly used to print monolayers of thiols on gold surfaces.[11,12] The sulfur atom binds to the gold surface and a dense self-assembled monolayer (SAM) is formed within seconds of contact time. However, μCP is not limited to printing thiols on gold. It has been shown that – subject to a suitable modification of stamp and substrate – virtually any type of ink can be patterned by μCP. The transfer of ink molecules from stamp to substrate is normally driven by a steep concentration gradient and it is favoured by weak adhesion to the stamp and strong chemisorption or physisorption to the substrate.

It was demonstrated in several early papers by Whitesides and coworkers that μCP can also be used to induce a chemical reaction between an ink and a reactive SAM. For example, amides are formed when amines are printed on an anhydride SAM on gold.[13] It must be noted that this observation is fully consistent with the rapid chemisorption in the contact area of stamp and substrate as well as with the inherent reactivity of amines and anhydrides. However, Huck and coworkers described the formation of peptides by printing N-protected amino acids onto an amine SAM on gold.[14] Of course, peptides do not spontaneously form from carboxylic acids and amines under ambient conditions, and it was proposed by Huck that "the nanoscale confinement of the ink at the interface between the stamp and the SAM, in combination with the pre-organization of the reactants in the SAM, facilitates the formation of covalent bonds". Subsequently, it was also shown that imines can be formed under ambient conditions by printing amines onto an aldehyde SAMs on gold.[15] This useful variation of μCP is also known as "reactive μCP"[13] or "microcontact chemistry".[16]

Recently, it was shown that also the Huisgen 1,3-dipolar cycloaddition of alkynes and azides can be induced by μCP.[17] Using a range of sensitive surface analysis methods (including infrared spectroscopy, X-ray photo-electron spectroscopy, atomic force microscopy, and fluorescence microscopy), it was shown that triazoles are formed within minutes when an alkyne is printed on an azide SAM on a Si wafer or glass, even in the absence of a Cu(I) catalyst that is normally used to accelerate this type of "click chemistry".[18] Click chemistry by μCP was then applied to print microarrays of alkyne-modified DNA[19] and alkyne-modified carbohydrates[20,21] on azide SAMs on Si wafers and glass. It was

---

Organic Chemistry Institute and CeNTech, Westfälische Wilhelms Universität Münster, Corrensstraße 40, 48149, Münster, Germany. E-mail: b.j.ravoo@uni-muenster.de; Fax: +49 251 83 36557

† Electronic supplementary information (ESI) available. See DOI: 10.1039/c1ob05187c

observed that although DNA could be printed without a Cu(I) catalyst, the surface density of carbohydrates was low in the absence of Cu(I) catalyst. Additionally, the heterogeneous catalysis of the cycloaddition of alkynes and azides by μCP was reported: a μCP stamp covered with a thin film of Cu (air-oxidized to Cu_2O) was used to induce the cycloaddition of alkynes on an azide SAM on gold.[22] It was demonstrated that the cycloaddition by μCP proceeds to completion (*i.e.* until all reactive sites on the surface are occupied) within a few hours when a Cu-coated stamp is used or Cu(I) catalyst is added to the alkyne ink. Recently also the Diels–Alder reaction as well as the photochemical thiol-ene/thiol yne reaction have been exploited to fabricate patterned arrays of carbohydrates by μCP.[23,24]

In this paper we report a structure–reactivity study of the Huisgen 1,3-dipolar cycloaddition, the Diels–Alder cycloaddition and the thiol-ene/yne reaction induced by μCP (Fig. 1). These reactions have found widespread use for the bio-orthogonal ligation of biomolecules to surfaces[25–28] and their combination with μCP results in an attractive method to prepare microarrays.[23,24] Our method of choice to investigate these surface reactions induced by μCP is fluorescence microscopy, since this is one of very few methods that are sensitive enough to detect the monolayer and sub-monolayer coverage of ink molecules on transparent substrates under ambient conditions. The intensity contrast between contact and non-contact regions serves as an internal reference in each printing experiment. Since the microscopy settings can be carefully controlled and reproduced, the intensity contrast can be taken as a quantitative measure for the surface coverage. In combination with a desorption experiment in which the fluorescent ink is removed from the surface, also the surface density (number of molecules per unit area) can be determined. The overall aim of this study is to gain insight into the kinetics of addition reactions on surfaces induced by μCP. In the first part of this paper we report a structure–reactivity study of the Huisgen 1,3-dipolar cycloaddition induced by μCP. In the second part, we investigate Diels–Alder reactions induced by μCP. Finally, in the third part we investigate thiol-ene and thiol-yne reactions induced by μCP.

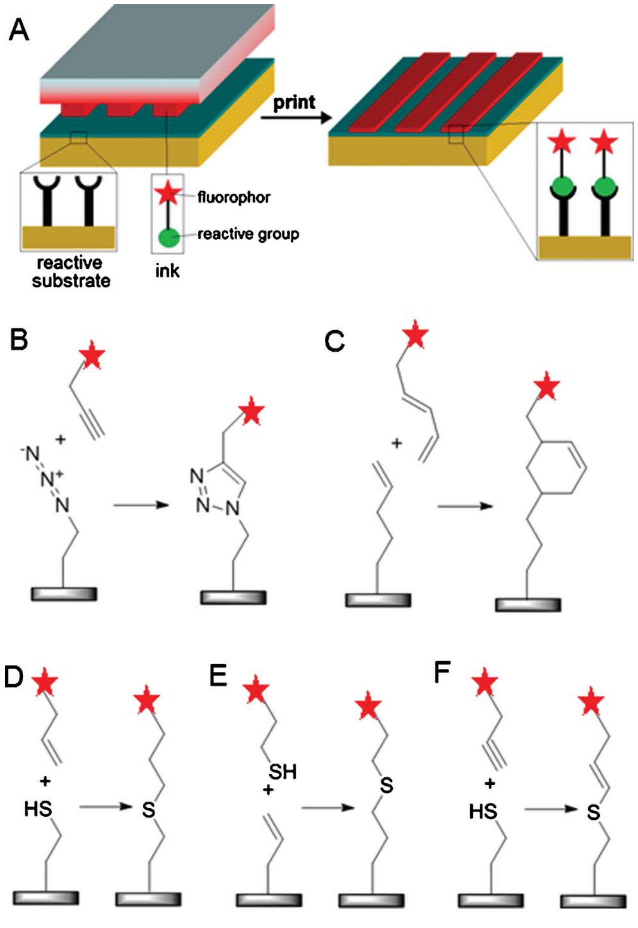

Fig. 1 A: Schematic illustration of the principle of microcontact chemistry: A fluorescent ink is printed on a substrate SAM and a reaction occurs exclusively in the area of contact. B: Huisgen 1,3-dipolar cycloaddition, C: Diels–Alder cycloaddition, D and E: Thiol-ene reaction, F: Thiol-yne reaction.

Results and discussion

1,3-Dipolar cycloaddition of alkynes and azides

In order to investigate the Huisgen 1,3-dipolar cycloaddition of alkynes and azides induced by μCP, a set of alkyne inks was synthesized (Scheme 1). The inks differ in the electron density of

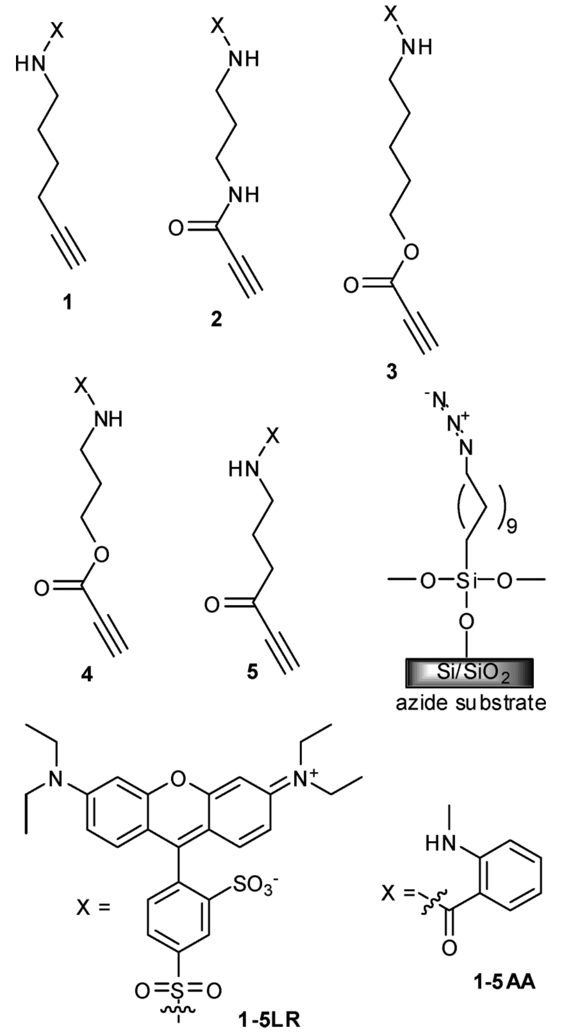

Scheme 1 Alkyne inks **1–5**, fluorescent labels and azide SAM used for the Huisgen 1,3-dipolar cycloaddition induced by μCP.

the terminal alkyne, which results in different inherent reactivity in the 1,3-dipolar cycloaddition with an aliphatic azide. According to the Frontier Molecular Orbital (FMO) description of this reaction an electron-rich alkyne (such as aliphatic alkyne **1**) is less reactive than an electron-poor alkyne conjugated to carbonyl groups such as amide **2**, esters **3** and **4**, and ketone **5**. Based on FMO arguments, it is expected that the order of reactivity of alkynes **1–5** with aliphatic azides is: $\mathbf{5} > \mathbf{4} \sim \mathbf{3} > \mathbf{2} \gg \mathbf{1}$.[29] All inks were labelled with a fluorophore so that they can be easily detected by fluorescence microscopy. To verify if the structure of the fluorophore affects the cycloaddition, inks **1–5** were labelled with the bulky, red-emitting lissamine rhodamine B (**1** – **5LR**) as well as with the compact, blue-emitting *N*-methylanthranyl amide (**1** – **5AA**). The synthesis of inks **1–5** is described in the ESI.†

The alkyne inks were printed on an azide-terminated SAM on glass. The azide SAM was prepared according to a literature procedure.[30] In short, a cleaned and activated microscopy cover slide was coated with a SAM of 11-bromoundecyltrichlorosilane. Formation of the 11-bromoundecylsilane SAM was followed by a substitution reaction with sodium azide. Due to the short immobilization time (20 min), the surface coverage of the 11-bromoundecylsilane SAM is substantially lower than a densely packed alkylsilane SAM. On the basis of literature data for the formation of octadecyltrichlorosilane SAMs, we estimate that the surface coverage of the 11-bromoundecylsilane SAM is around 1 molecule/nm^2 or 1×10^{14} molecules/cm^2.[31,32,33] The advantage of a lower density of reactive groups is a reduced steric hindrance, a better access for incoming reagents, and hence a more rapid conversion than would be expected for a densely packed SAM.

Elastomeric polydimethylsiloxane (PDMS) stamps for µCP were prepared according to established procedures (see experimental section for details). Stamps of 1×1 cm^2 were structured with stripes in two different dimensions due to the design of the available master (5 µm width and 3 µm interspace or 10 µm width and 5 µm interspace). The microstructure of the stamp did not give rise to significant differences during printing. In view of the polarity of the ink molecules, the PDMS stamps were activated by oxidation in an ozone generator prior to printing. Oxidation of the PDMS surface results in significantly increased adsorption of the ethanolic ink solution to the stamp surface, and hence enhanced transfer of ink molecules from the stamp to the substrate during printing.[8–10]

All alkyne inks were printed and imaged under identical conditions: inking time 1 min, ink concentration 1 mM in ethanol, 20 g weight during printing, identical rinsing procedure following printing, identical microscopy and camera settings. The only variable parameters were the structure of the ink and the printing time. Fig. 2 shows a set of images obtained by printing alkyne **1LR** on an azide SAM substrate for different printing times as well as the brightness contrast between contact and non-contact area observed for each printing time. The brightness of the stripes in the contact area was taken as a measure for the amount of ink that reacted on the substrate during printing. The dark area in between the stripes (*i.e.* the non-contacted area) is taken as internal reference. This experimental procedure was repeated several times for all rhodamine inks **1** – **5LR** in order to exclude experimental errors. In addition, ink **1LR** was also printed in the presence of catalytic amounts of Cu(I) in the ethanolic ink solution. The results are summarised in a plot of brightness contrast against printing time in Fig. 3.

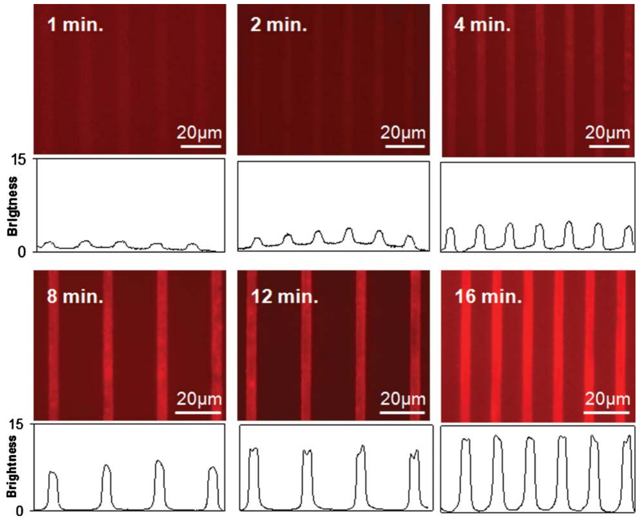

Fig. 2 Microscopy images and contrast profiles for printing fluorescent alkyne **1LR** on an azide SAM for increasing printing time.

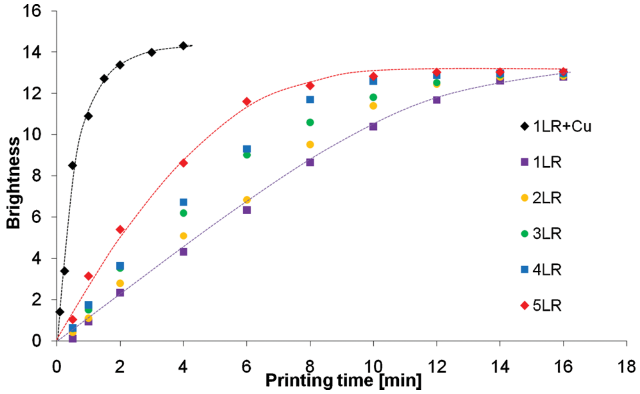

Fig. 3 Alkyne inks 1-5LR and 1LR + Cu(I) printed on azide SAMs. Printing time dependence of the fluorescence intensity. All printing experiments were carried out under identical conditions. Trend lines serve to guide the eye.

A clear trend is obvious from the curves collected in Fig. 3. First of all, it is reasonable to assume that the fluorescence brightness contrast scales with the surface density of fluorescent molecules on the surface. In line with this assumption, all curves for inks **1** – **5LR** display a similar maximum intensity contrast, which may be taken as the maximum coverage of alkyne molecules that can be immobilized on the azide SAM by µCP. Furthermore, it is clear from Fig. 2 that all surface reactions induced by µCP are complete within 15 min. However, a distinct reactivity trend of the inks ($\mathbf{1} < \mathbf{2} < \mathbf{3} \approx \mathbf{4} < \mathbf{5}$) is also evident, demonstrating that the cycloaddition induced by µCP follows the trend predicted by FMO theory. Moreover, the reaction of **1LR** in the presence of Cu(I) catalyst is much faster than all other reactions, but the maximum density of fluorescent molecules on the surface is not significantly higher. Obviously the limiting factor also in this "click" immobilization reaction is the availability of azide on the substrate. To aid a straightforward comparison, the reactivity curves in Fig. 3 were converted into an approximate half life of the µCP induced cycloaddition, assuming pseudo first order kinetics for the reaction of the azide SAM with an excess of alkyne ink on the stamp. The half life of the cycloaddition for each ink is

Table 1 Half life (min) of the reactions of alkyne inks **1–5LR** and **1–5AA** on azide SAMs

	1	**2**	**3**	**4**	**5**	**1 + Cu(I)**
RL	6.3	5.7	4.3	3.8	2.8	0.4
AA	6.6	5.9	4.2	3.9	3.0	0.5

listed in Table 1. From Table 1 it can be seen that for example ketone **5** reacts approximately 2 times faster than aliphatic alkyne **1**, and that the addition of Cu(I) catalyst to alkyne **1** leads to an acceleration of the cycloaddition by a factor of 15. Finally, in order to exclude effects of the bulky rhodamine fluorescent label on the cycloaddition by μCP, the same experiments were carried out with the inks **1–5AA**, equipped with a much smaller fluorescent N-methylanthranyl amide label. By using the experimental protocol described above, the half life for the μCP induced cycloaddition reactions of the blue alkyne inks can be obtained. They are also shown in Table 1. The similarity of the results is obvious from the half life. We conclude that the fluorescent labels do not affect the surface reaction.

Diels–Alder reaction

We also performed a reactivity study of the Diels–Alder reaction induced by μCP of fluorescent dienes on alkene SAMs using a similar procedure as described above for the 1,3-dipolar cycloaddition. However, in this case not only the reactivity of the ink molecules but also the reactivity of the substrates was varied systematically. Depending on the nature of the diene and dienophile, the Diels–Alder reaction can be reversible and much more temperature dependent than the 1,3-dipolar cycloaddition of alkynes and azides. Diene derivatives **6**, **7** and **8** were used as molecular inks (Scheme 2). These dienes were labelled with rhodamine lissamine B. The synthesis of inks **6–8** is described in the ESI.† In a normal electron demand Diels–Alder reaction, furan **6** should have the lowest reactivity, pentadiene **7** should have intermediate reactivity, and cyclopentadiene **8** should have the highest reactivity towards a given dienophile.[34,35] As a substrate for μCP, SAMs terminated with an alkene (**9**) and an acrylamide (**10**) were prepared (see experimental section). Alkene SAM **9** was prepared directly from 7-octenyltriethoxysilane. Acrylamide SAM **10** was prepared in a three step procedure by reduction of an azido SAM (see above) followed by reaction with acryloylchloride. The surface coverage of these SAMs is around 1×10^{14} molecules/cm^2.[31,32,33]

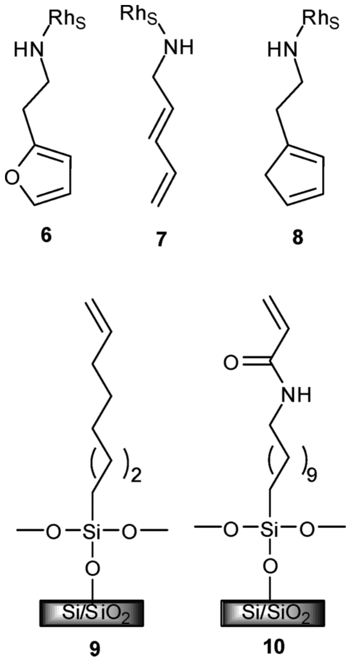

Scheme 2 Diene inks and dienophile SAMs used for Diels–Alder reactions induced by μCP.

Table 2 Half life (min) of the reactions of diene inks **6–8** on dienophile SAMs **9** and **10**

	6	**7**	**8**
9	>20	9.4	5.5
10	16.3	6.0	4.7

As described above for the 1,3-dipolar cycloaddition, all diene inks were printed and imaged under identical conditions: inking time 1 min, ink concentration 1 mM in ethanol, 20 g weight during printing, identical rinsing procedure following printing, identical microscopy and camera settings. The only variable parameter was the structure of the ink, the substrate SAM, and the printing time. After printing each ink **6–8** the substrate was carefully rinsed and fluorescence images were evaluated. The brightness of the stripes in the contact area was taken as a measure for the amount of diene ink that reacted on the dienophile surface during printing. The dark area in between the stripes (*i.e.* the non-contacted area) is taken as internal reference. The observed brightness contrast as a function of printing time is shown for μCP of dienes **6–8** on alkene SAM **9** in Fig. 4. It can be seen from Fig. 4 that the Diels–Alder reaction of dienes **6–8** with SAM **9** follows the reactivity trend predicted by FMO theory (**8** > **7** > **6**). However, no maximum contrast is reached within 20 min for any of the inks, indicating that these Diels–Alder reactions proceed significantly slower than the Huisgen 1,3-dipolar cycloadditions described above. Longer printing times are not practical in view of ink diffusion into the non-contacted area. Table 2 displays the results in terms of an approximate half life for the Diels–Alder reactions by μCP. The maximum contrast obtained for **8** printed on **9** was taken as reference for complete conversion.

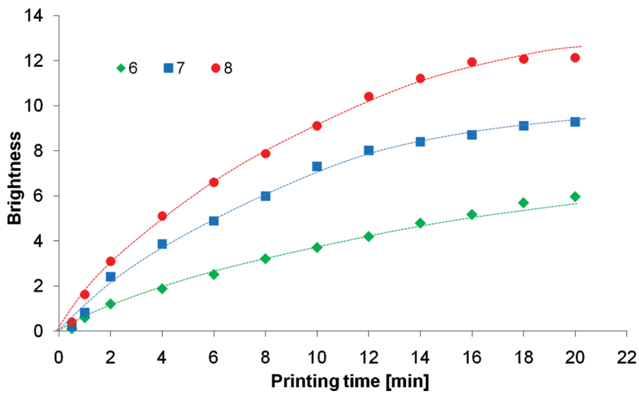

Fig. 4 Diene inks **6–8** printed on dienophile SAM **9**. Printing time dependence of the fluorescence intensity. All printing experiments carried out under identical conditions. Trend lines serve to guide the eye.

A comparable result is obtained when the substrate instead of the ink is varied in reactivity. Fig. 5 shows the increase in contrast with time resulting from printing pentadiene **7** on substrate SAMs **9** and **10**. Although the differences are modest, a significantly higher reactivity can be observed for **10**. These experiments are also included in Table 2 in terms of an approximate half life for the Diels–Alder reaction by μCP.

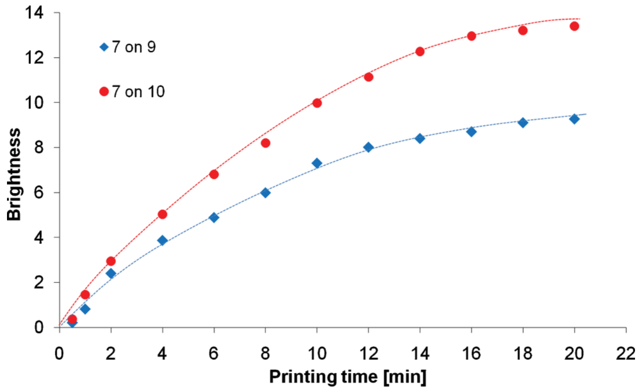

Fig. 5 Diene ink **7** printed on dienophile SAMs **9** and **10**. Printing time dependence of the fluorescence intensity. All printing experiments carried out under identical conditions.

A comparison of each of the three diene inks printed on each of the dienophile SAMs can be made on the basis of the approximate half life to reach maximum surface coverage. To calculate the half life, the maximum contrast obtained for diene **8** printed on dienophile **10** was taken as reference since this was the combination of ink and substrate that gave the highest fluorescence contrast, *i.e.* the highest surface density of ink, as a result of a rapid Diels–Alder reaction between electron-rich cyclopentadiene **8** printed on electron-poor acrylamide SAM **10**. It can be seen from Table 2 that furan **6** reacts only slowly with any of the dienophile SAMs **9** and **10**. We note that these findings are fully in line with FMO theory as well as experimental rate constants of Diels–Alder reactions in solution.[34,35]

Temperature dependence and retro-Diels–Alder reaction

The temperature dependence of the Huisgen 1,3-dipolar cycloaddition as well as the Diels–Alder reaction induced by μCP was investigated by printing alkyne **1** on an azide SAM and by printing pentadiene **7** on alkene SAM **9** at a range of temperatures (Fig. 6). The printing time was 10 min in each case. It can clearly be observed that there is a strong temperature effect on the Diels–Alder reaction whereas the μCP-induced 1,3-dipolar cycloaddition is hardly influenced. This finding is in accordance with the literature on the corresponding reactions in solution.[29,34,35] The absence of a large temperature effect on the 1,3-dipolar cycloaddition also demonstrates that the temperature effect on the Diels–Alder reaction cannot be explained by temperature effects on the μCP process, such as faster diffusion of the ink at higher temperature.

The reversibility of the Diels–Alder reaction can be exploited to perform a second type of reactivity study. To this end, diene inks **6–8** were printed for 30 min on alkene substrates **9**, rinsed as usual and then dipped into boiling ethanol. Fig. 7 shows the results for **7** printed on **9** as an example. The bright fluorescent stripes

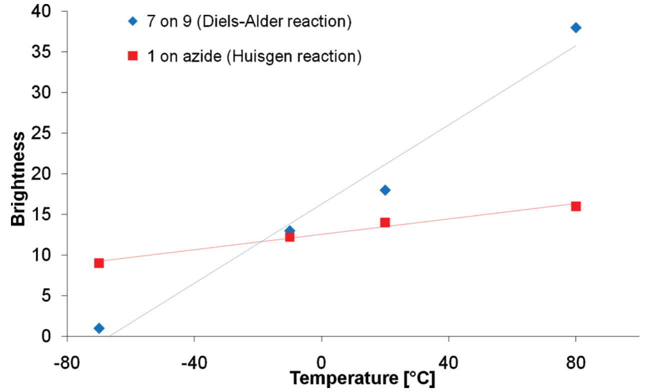

Fig. 6 Temperature dependence of a Diels–Alder reaction (diene ink **7** printed on dienophile SAM **9**) and 1,3-dipolar cycloaddition (alkyne ink **1** printed on azide SAM), printed for 10 min in all cases. Trend lines serve to guide the eye.

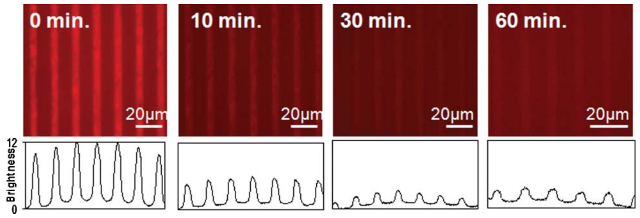

Fig. 7 Fluorescence images and contrast profiles for diene **7** printed on dienophile SAM **9** for 30 min followed by treatment with boiling ethanol for 10, 30 and 60 min.

(*i.e.* cycloaddition product obtained by μCP) become less and less fluorescent the longer they are treated with boiling ethanol. This observation implies that the surface density of fluorescent ink decreases with time. The desorption of ink in boiling ethanol can be readily explained by a retro–Diels–Alder reaction. The rate of the reverse reaction is different for the three diene inks (Fig. 8). Whereas the Diels–Alder reaction is completely reversible within 10 min in boiling ethanol for furan **6** printed on SAM **9**, it is hardly reversible for cyclopentadiene **8**. We note that also these findings are fully in line with FMO theory.

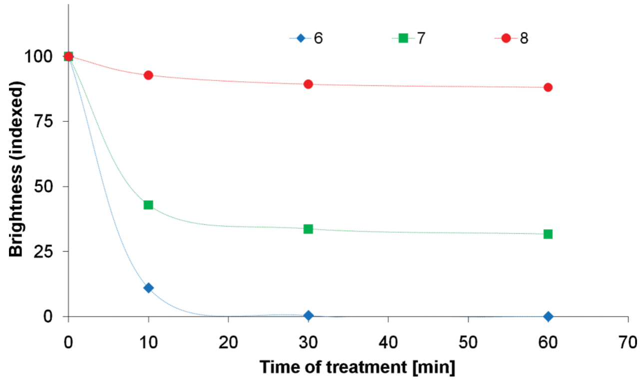

Fig. 8 Retro–Diels–Alder reaction in boiling ethanol of dienes **6–8** printed on dienophile SAM **9**. Trend lines serve to guide the eye.

The reversibility of the Diels–Alder reaction was exploited in order to determine the surface density of printed diene ink. After printing diene **7** with a large, flat, unstructured stamp on an alkene SAM **9** on a substrate with defined size (1.8 × 1.8 cm, 3.24 cm^2) and extensive rinsing with cold ethanol, the retro–Diels–Alder reaction was induced by treating the samples with boiling ethanol. The concentration of rhodamine desorbed from the substrate was measured with a fluorescence spectrometer and compared to a calibration curve for rhodamine solutions with known concentrations. It was found that on average 4 nmol or 6×10^{13} fluorescent molecules desorbed from the substrate. Assuming that this number equals the number of diene molecules that were attached to the alkene surface as a result of µCP, the surface density of immobilized ink was 1.8×10^{13} molecules/cm^2. As discussed above, the surface density of the substrate SAM was around 1×10^{14} molecules/cm^2. Hence, µCP results in the formation of a rather dense layer of cycloaddition product on top of the substrate SAM. It is likely that the density of the cycloaddition product is limited by the size and polarity of the rhodamine inks rather than the surface coverage of the reactive groups on the substrate SAM.

Unfortunately the desorption experiment cannot be performed for the 1,3-dipolar cycloaddition because this reaction is not thermally reversible. However, if one compares (under identical microscopy and camera settings) the maximum brightness obtained when printing alkynes on azide SAMs with the maximum obtained when printing dienes on dienophile SAMs, it appears that the surface coverage as a result of the 1,3-dipolar cycloaddition is even higher than the surface coverage as a result of the DA reaction. Hence, there is no doubt that µCP induced 1,3-dipolar cycloadditions results in a dense microarray of cycloaddition product, even in the absence of Cu(I) catalyst.[22]

Thiol-ene and thiol-yne reaction

The photo-induced thiol-ene addition reaction (and to a lesser extent, the thiol-yne reaction) has had a major impact on chemistry and materials science in the last few years.[36] We have recently shown that these reactions can also be used to prepare microarrays by photochemical µCP.[24] In this article, we report a structure–reactivity study for a range of thiols and alkenes or alkynes undergoing a photo-induced thiol-ene or thiol-yne reaction, respectively. An interesting aspect of this particular addition reaction is to verify whether it can be induced by µCP without UV irradiation, similar to the rapid Huisgen 1,3-dipolar cycloaddition without Cu(I) induced by µCP. To this end, fluorescent thiols were printed on alkene SAMs and fluorescent alkenes were printed on thiol SAMs. Scheme 3 shows an overview of all used inks and SAMs investigated in thiol-ene reactions induced by µCP. The synthesis of inks **7** and **11–14** is described in the ESI.†

Alkene inks **7**, **11** and **12** were printed onto thiol SAM **15**. Furthermore, thiol inks **13** and **14** were printed onto alkene SAM **16**. The experimental procedure was essentially the same as described for the cycloaddition reactions described above. However, an UV diode with maximum emission at 365 nm was placed in a small chamber with the printing setup and the interface of stamp and substrate was irradiated during printing. Fig. 9 shows the results of printing inks **7**, **11**, and **12** onto SAM **15**. Allylic ink **11** is expected to be the least reactive ink, acrylic ester ink **12** is the most reactive, while reactivity of the conjugated diene **7** is between the other two.[37] This is found also in this study and can be quantified by an approximate half life (2.0 min for **11**, 0.9 min for **12**, 1.2 min for **7**).

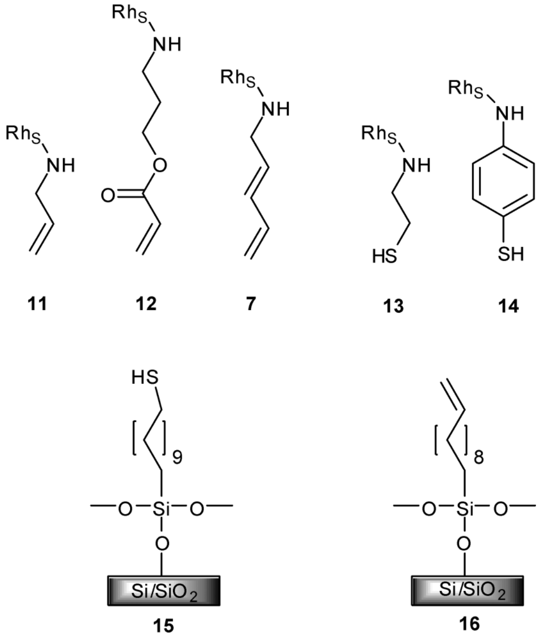

Scheme 3 Inks and SAMs used for thiol-ene reactions induced by µCP.

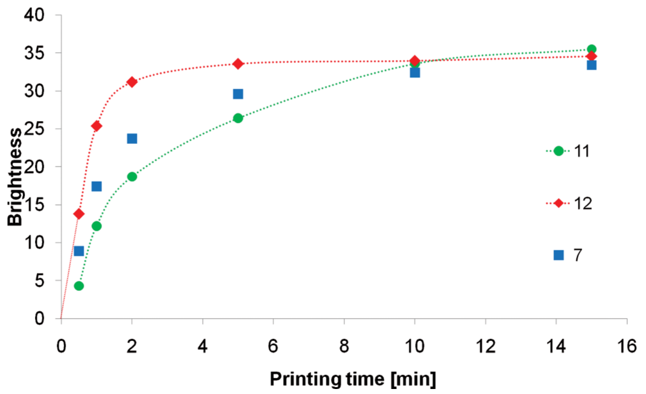

Fig. 9 Alkene inks **7**, **11** and **12** printed on thiol SAM **15**. Printing time dependence of the fluorescence intensity. All printing experiments carried out under UV irradiation. Trend lines serve to guide the eye.

Printing the thiol inks **13** and **14** onto alkene SAM **16** also showed a structure–reactivity relationship as expected. No significant difference between the reaction rate of aminoethanethiol **13** and aminothiophenol **14** could be observed: the thiol-ene reaction proceeds very fast in either case (Fig. 10). Ink **14** was printed on alkene SAM **16** using various irradiation conditions. Under irradiation with UV light the reaction rate is high as expected, at ambient light conditions the yield is still remarkably high, while in the dark the reaction proceeds only very slowly (Fig. 10).

Finally, the alkyne inks **1–5** used for the investigation of the Huisgen 1,3-dipolar cycloaddition were used for the thiol-yne reaction by printing them onto thiol SAM **15**. Their relative reactivity is the same in both reactions, *i.e.* electron-poor alkynes react faster than electron-rich alkynes (**5** > **4** ~ **3** > **2** ≫ **1**). The results of the printing experiments are summarised in Fig. 11. Although a trend confirming the expected structure–reactivity relationship is visible, it was found that all reactions proceed rapidly to completion. In every case, the half life is less than 1 min and it is difficult to quantify the reactivity of the alkynes.

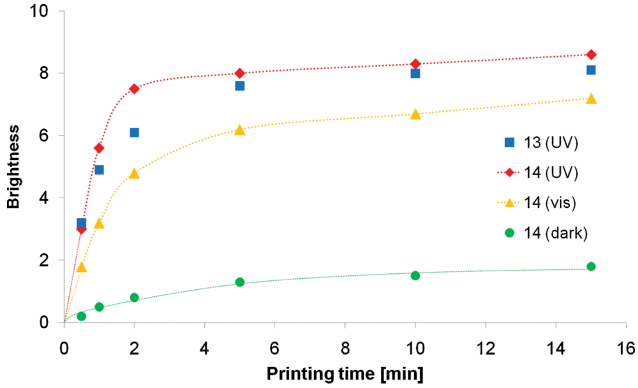

Fig. 10 Thiol inks **13** and **14** printed onto alkene SAM **16**. Printing time dependence of the fluorescence intensity under varying light conditions. Trend lines serve to guide the eye.

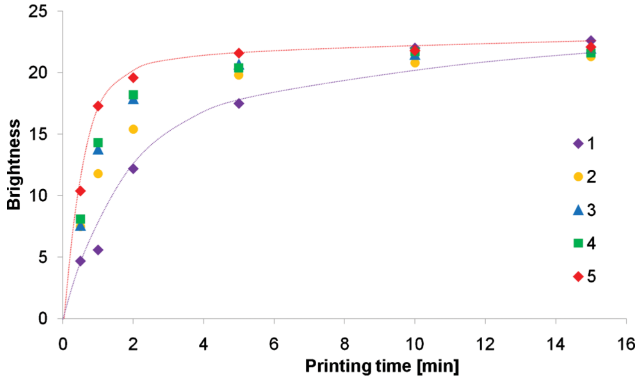

Fig. 11 Alkyne inks **1–5** printed on thiol SAM **15**. Printing time dependence of the fluorescence intensity. All printing experiments carried out under UV irradiation. Trend lines serve to guide the eye.

Conclusion

The Huisgen 1,3-dipolar cycloaddition, Diels–Alder cycloaddition, and thiol-ene/yne reaction can be induced by µCP of alkynes on an azide SAM, dienes on a dienophile SAM, and thiols on an alkene or alkyne SAM (and *vice versa*), respectively. All three addition reactions result in a dense surface coverage within a few minutes, but reaction by µCP is fastest for the most reactive reagent pairs. The Huisgen 1,3-dipolar cycloaddition can be significantly accelerated by Cu(I) catalysis while the thiol-ene/yne addition is particularly effective under UV irradiation. Under optimized conditions, the Cu(I) catalyzed 1,3-dipolar cycloaddition of alkynes and azides and the photo-induced thiol-ene/yne reactions are substantially faster than the Cu(I)-free Huisgen cycloaddition and the Diels–Alder reaction. The characteristic structure–reactivity relationships of the addition reactions as well as the retro-Diels–Alder reaction can be taken as evidence that in all cases a chemical reaction (rather than physisorption) is induced by µCP. In many respects, reactions induced by µCP follow the principles of click chemistry (*i.e.* near-quantitative yield, mild reaction conditions, and short reaction time) and thus provide a straightforward method for the fabrication of (bio)molecular microarrays for a range of applications.

Experimental section

Ink synthesis

Fluorescent alkyne, diene, alkene and thiol derivatives were synthesised following literature methods. Experimental details and spectroscopic data are provided in the ESI.†

Surface modification

The azide terminated SAM was obtained following a method first described by Balachander and Sukenik.[30] A glass substrate (microscopy cover slides, servoprax®, Wesel (Germany)) was cleaned and activated by treatment with hot "piranha" solution (conc. H_2SO_4/30% H_2O_2, 3 : 1) for at least 30 min. The substrate was dipped into a solution of 11-bromoundecyltrichlorosilane (ABCR) in toluene (0.1%) for 20 min at room temperature followed by storing the dried substrates at 80 °C for at least 2 h. The samples are then brought into a saturated solution of NaN_3 in DMF at 70 °C for 48 h. After sonication for 30 s and rinsing with ethanol the substrates are dried and stored in air-tight boxes. The quality of the monolayer formation and transformation was verified by contact angle measurements (adv. angle (lit.): 82° ± 2 (77° ± 2),[30] rec. angle (lit.): 74° ± 2 (71° ± 2)[30]).

The alkene terminated SAMs **9** and **16** were formed by dipping the piranha-treated glass substrates into a 0.1% solution of 7-octenyltriethoxysilane (ABCR), or 10-undecenyltrichlorosilane, respectively, in toluene for 2 h at 50 °C. Contact angle: adv. (lit.): 115° ± 3 (111° ± 4),[23] rec. (lit.): 91° ± 2 (88° ± 3).[23]

To obtain the alkene terminated amide SAM **10**, an azide terminated SAM was reduced to an amine SAM with a solution of PPh_3 in dry THF (0.1 M) for 3 h and then dipped into a solution of acrylic acid (0.02 M), DCC (9.5mM) and a catalytic amount of DMAP in ethyl acetate for 48 h at RT. Contact angle: adv.: 117° ± 4, rec.: 77° ± 4.

Thiol terminated SAM **15** was prepared following a protocol by Balachander and Sukenik.[30] Piranha-activated glass substrates are equipped with a monolayer of 11-bromoundecyltrichlorosilane by dipping them into a solution of that substance in toluene (0.1%) for 20 min at room temperature followed by storing the dried substrates at 80 °C for at least 2 h. These substrates are dipped into a solution of potassium thiocyanate in DMF (10 mg mL^{-1}) for 20 h. The resulting SCN-terminated monolayer was transformed to a thiol-SAM by treatment with $LiAlH_4$ for 4 h. Contact angle: adv. (lit.): 72° ± 2 (71° ± 3),[30] rec. (lit.): 45° ± 4 (49° ± 3).[30]

PDMS stamps

The PDMS stamps were prepared by mixing PDMS (obtained from Dow Corning® as Sylgard 184) with a curing agent (10 : 1) followed by degassing and pouring the bubble free mixture onto a 4″ silicon wafer carrying 24 8 × 8 mm areas of the desired pattern (produced by common photolithographic methods). The prepolymer was hardened by baking it overnight at 70 °C and the stamp was peeled off the master carefully. After cutting it into the 24 single stamps these were oxidised in an UV/ozone generator (Novascan PSD-UV) and stored in MilliQ water to prevent hydrophobic recovery.

Printing procedure

The dry stamp was inked for 1 min by placing drops of ink on the patterned side of the stamp or by dipping the stamp into ink solution. The stamp was dried with compressed air and placed with the patterned side onto the cleaned and dried substrate. After contact any further movement is avoided. A weight of 20 g is put on top of the stamp to ensure conformal contact. After the desired printing time the stamp plus weight was removed in one move. The substrate was rinsed vigorously with ethanol, sonicated for 30 s and rinsed again with ethanol to remove all physisorbed ink and contamination. The printed substrates were investigated with a fluorescence microscope (Olympus) and micrographs are taken with a digital camera (Kappa). Identical parameter settings (exposure time 990 ms, gain 180, Gamma 100) are used in order to obtain images that can be quantitatively compared and evaluated with ImageJ software. Printing at different temperatures was carried out on a metal plate placed on a isopropanol/dry ice mixture (−80 °C), on a ice/salt mixture (−15 °C) or on paraffin oil heated to 70 °C. The substrate was placed on the plate for several min to make sure it has the same temperature as the plate. For temperatures below 0 °C condensation of water was avoided by placing the setup in dry argon atmosphere.

Retro-Diels–Alder reaction

After printing the inks on the SAMs according to the standard procedure described above for 30 min and taking the fluorescence images the samples are dipped into boiling ethanol. After 10, 30 and 60 min of treatment the samples are taken out, rinsed with ethanol, dried and investigated with fluorescence microscopy.

Surface density determination

Pentadiene ink **7** was printed on alkene SAM **9** (18 × 18mm glass slide) with a flat stamp bigger than the slide for 30 min. The substrate was rinsed vigorously with ethanol and sonicated for 30 s. The substrate is placed in approx. 15 mL boiling ethanol under reflux for 2 h, then taken out and rinsed with a small amount of ethanol which is added to the boiling ethanol. The exact volume of this solution is determined and then the fluorescence intensity at 585 nm ($\lambda_{\max}$ of rhodamine lissamine B) is measured with a fluorescence spectrometer and compared to a calibration curve which is obtained from solutions with known concentrations of lissamine rhodamine B.

Acknowledgement

The authors are grateful for financial support by the Deutsche Forschungsgemeinschaft (IRTG 1143 Münster-Nagoya).

References

1 R. J. Hamers, *Annu. Rev. Anal. Chem.*, 2008, **1**, 707–736.
2 A. Natan, L. Kronik, H. Haick and R. T. Tung, *Adv. Mater.*, 2007, **19**, 4103–4117.
3 D. B. Weibel, P. Garstecki and G. M. Whitesides, *Curr. Opin. Neurobiol.*, 2005, **15**, 560–567.
4 M. J. W. Ludden, J. K. Sinha, G. Wittstock, D. N. Reinhoudt and J. Huskens, *Org. Biomol. Chem.*, 2008, **6**, 1553–1557.
5 K. Ichimura, S. K. Oh and M. Nakagawa, *Science*, 2000, **288**, 1624–1626.
6 M. Kleinert, T. Winkler, A. Terfort and T. K. Lindhorst, *Org. Biomol. Chem.*, 2008, **6**, 2118–2132.
7 Y. Xia and G. M. Whitesides, *Angew. Chem., Int. Ed.*, 1998, **37**, 550.
8 S. A. Ruiz and C. S. Chen, *Soft Matter*, 2007, **3**, 168.
9 A. Perl, D. N. Reinhoudt and J. Huskens, *Adv. Mater.*, 2009, **21**, 2257.
10 T. Kaufmann and B. J. Ravoo, *Polym. Chem.*, 2010, **1**, 371.
11 A. Kumar and G. M. Whitesides, *Appl. Phys. Lett.*, 1993, **63**, 2002–2004.
12 J. L. Wilbur, A. Kumar, E. Kim and G. M. Whitesides, *Adv. Mater.*, 1994, **6**, 600–604.
13 L. Yan, W. T. S. Huck, X. M. Zhao and G. M. Whitesides, *Langmuir*, 1999, **15**, 1208–1214.
14 T. P. Sullivan, M. L. van Poll, P. Y. W. Dankers and W. T. S. Huck, *Angew. Chem., Int. Ed.*, 2004, **43**, 4190–4193.
15 D. I. Rozkiewicz, B. J. Ravoo and D. N. Reinhoudt, *Langmuir*, 2005, **21**, 6337.
16 B. J. Ravoo, *J. Mater. Chem.*, 2009, **19**, 8902–8906.
17 D. I. Rozkiewicz, D. Jancewski, W. Verboom, B. J. Ravoo and D. N. Reinhoudt, *Angew. Chem., Int. Ed.*, 2006, **45**, 5292.
18 H. C. Kolb, M. G. Finn and K. B. Sharpless, *Angew. Chem., Int. Ed.*, 2001, **40**, 2004–2021.
19 D. I. Rozkiewicz, J. Gierlich, G. A. Burley, K. Gutsmiedl, T. Carell, B. J. Ravoo and D. N. Reinhoudt, *ChemBioChem*, 2007, **8**, 1997–2002.
20 O. Michel and B. J. Ravoo, *Langmuir*, 2008, **24**, 12116–12118.
21 K. Godula, D. Rabuka, K. Nam and C. R. Bertozzi, *Angew. Chem., Int. Ed.*, 2009, **48**, 4973–4976.
22 J. M. Spruell, B. A. Sheriff, D. I. Rozkiewicz, W. R. Dichtel, R. D. Rohde, D. N. Reinhoudt, J. F. Stoddart and J. R. Heath, *Angew. Chem., Int. Ed.*, 2008, **47**, 9927–9932.
23 C. Wendeln, A. Heile, H. F. Arlinghaus and B. J. Ravoo, *Langmuir*, 2010, **26**, 4933–4940.
24 C. Wendeln, S. Rinnen, C. Schulz, H. F. Arlinghaus and B. J. Ravoo, *Langmuir*, 2010, **26**, 15966–15971.
25 A. D. de Araujo, J. M. Palomo, J. Cramer, M. Kohn, H. Schroder, R. Wacker, C. M. Niemeyer, K. Alexandrov and H. Waldmann, *Angew. Chem., Int. Ed.*, 2006, **45**, 296–301.
26 P. Jonkheijm, D. Weinrich, M. Koehn, H. Engelkamp, P. C. M. Christianen, J. Kuhlmann, J. C. Maan, D. Nuesse, H. Schroeder, R. Wacker, R. Breinbauer, C. M. Niemeyer and H. Waldmann, *Angew. Chem., Int. Ed.*, 2008, **47**, 4421–4424.
27 L. S. Wong, F. Khan and J. Micklefield, *Chem. Rev.*, 2009, **109**, 4025–4053.
28 N. Gupta, B. F. Lin, L. Campos, M. D. Dimitriou, S. T. Hikita, N. D. Treat, M. V. Tirrell, D. O. Clegg, E. J. Kramer and C. J. Hawker, *Nat. Chem.*, 2010, **2**, 138–145.
29 R. Huisgen, *Angew. Chem.*, 1963, **75**, 742–754.
30 N. Balachander and C. N. Sukenik, *Langmuir*, 1990, **6**, 1621–1627.
31 S. Semal, M. Voue', M. J. de Ruijter, J. Dehuit and J. De Coninck, *J. Phys. Chem. B*, 1999, **103**, 4854–4861.
32 Y. Liu, L. K. Wolf and M. C. Messmer, *Langmuir*, 2001, **17**, 4329–4335.
33 S. Onclin, B. J. Ravoo and D. N. Reinhoudt, *Angew. Chem., Int. Ed.*, 2005, **44**, 6282–6304.
34 V. D. Kiselev and A. I. Konovalov, *J. Phys. Org. Chem.*, 2009, **22**, 466–483.
35 J. Sauer and R. Sustmann, *Angew. Chem., Int. Ed. Engl.*, 1980, **19**, 779–807.
36 C. E. Hoyle and C. N. Bowman, *Angew. Chem., Int. Ed.*, 2010, **49**, 1540–1573.
37 K. Griesbaum, *Angew. Chem.*, 1970, **82**, 276–287.